Effects of Band Filling on Magnetic Structures: The Case of $R\mathrm{Ni_2Ge_2}$

Zahirul Islam,[1,*] C. Detlefs,[1,†] C. Song,[1] A. I. Goldman,[1] V. Antropov,[1] B. N. Harmon,[1]
S. L. Bud'ko,[1] T. Wiener,[1] P. C. Canfield,[1] D. Wermeille,[2] and K. D. Finkelstein[3]
[1]*Ames Laboratory and Department of Physics and Astronomy, Iowa State University, Ames, Iowa 50011*
[2]*Liquid Crystal Institute, Kent State University, Kent, Ohio 44242*
[3]*Cornell High Energy Synchrotron Source, Cornell University, Ithaca, New York 14853*
(Received 22 April 1999)

We establish that strong Fermi surface nesting drives the Néel transition in the $R\mathrm{Ni_2Ge_2}$ compounds. Generalized susceptibility, $\chi_0(\mathbf{q})$, calculations found nesting to be responsible for both *incommensurate* wave vector, (0 0 0.793), in $\mathrm{GdNi_2Ge_2}$, and the *commensurate* structure, (0 0 1), in $\mathrm{EuNi_2Ge_2}$, as revealed by x-ray resonant exchange scattering. A continuous transition from incommensurate to commensurate magnetic structures via band filling is predicted. The surprisingly higher T_N in $\mathrm{EuNi_2Ge_2}$ than that in $\mathrm{GdNi_2Ge_2}$ is also explained.

PACS numbers: 75.10.–b, 75.25.+z, 75.30.–m, 78.70.Ck

Rare-earth intermetallics with the tetragonal $\mathrm{ThCr_2Si_2}$ structure have been the subject of intensive study for several decades because of their intricate magnetic structures and various correlated electron phenomena [1]. The complex crystal structure and multiatom composition of these materials, relative to the elemental rare-earth metals, result in more involved band structures and magnetic interactions. While experimental studies of their magnetism have focused on the determination of ordered states, a quantitative theoretical understanding of their magnetic phase transition is lacking. In earlier work [2] on $R\mathrm{Ni_2Ge_2}$ compounds it was noted that, at the onset of antiferromagnetic (AF) ordering in the Pr, Nd, Sm, and Tb through Tm members of the series, there is an *incommensurate* magnetic modulation of the form $\mathbf{q} = (0\ 0\ q_z)$ with q_z in the range of $(0.75-0.81)\,(\frac{2\pi}{c})$, where c is the axial lattice parameter. The persistence of a single incommensurate $\mathbf{q}$ along the high-symmetry Λ line across the series is similar to the case of the elemental rare earths (Tb-Tm) [3]. In these intermetallic systems with low ordering temperatures ($\lesssim$30 K), the R atoms are well separated ($\gtrsim$4 Å) from each other. Thus, the indirect Ruderman-Kittel-Kasuya-Yosida (RKKY) exchange interaction, via the conduction electron polarization, is believed to be responsible for their magnetic ordering.

In this Letter we establish, both experimentally and computationally, a direct correlation between the magnetic order found in the $R\mathrm{Ni_2Ge_2}$ compounds and their underlying electronic structure by studying two particularly interesting members of this family, $\mathrm{GdNi_2Ge_2}$ and $\mathrm{EuNi_2Ge_2}$, respectively. We show that there exists strong Fermi surface nesting with $\mathbf{q}_{\mathrm{nest}} = (0\ 0\ q_z)$ and that it is possible to *transform* the ordered state via band filling in a *predictable* way. In addition, both the larger generalized electronic susceptibility, $\chi_0(\mathbf{q})$, and an increased $5d$ character of the electronic wave functions that nest were found to be responsible for the higher Néel temperature (T_N) observed in $\mathrm{EuNi_2Ge_2}$ compared to that of $\mathrm{GdNi_2Ge_2}$. This is in direct contrast to the expectation of a lower T_N in $\mathrm{EuNi_2Ge_2}$ due to weaker $4f$-$5d$ exchange interaction in atomic Eu compared to that in Gd [4].

The isostructural $\mathrm{GdNi_2Ge_2}$ and $\mathrm{EuNi_2Ge_2}$ compounds are ideal systems for the study of effects of band filling on magnetic structures since, in these compounds at ambient pressure, Gd and Eu are *trivalent* and *divalent*, respectively [5,6]. Therefore, due to their half-filled $4f$ shells, the Hund's rule ground state is ${}^8S_{7/2}$ which gives an isotropic magnetic moment unaffected by the crystal fields. The RKKY exchange is the only relevant interaction determining magnetic order for these compounds. An incommensurate ordering vector, as observed for the trivalent members of the series, is expected for the Gd compound. However, due to the divalency of Eu in $\mathrm{EuNi_2Ge_2}$, its magnetic structure, in particular the modulation vector, is expected to be significantly different since the RKKY interactions should be dramatically influenced by lower band filling. Theoretically, it is possible to correlate these differences to the underlying electronic structures using band structure and $\chi_0(\mathbf{q})$ calculations.

High-quality single crystals [7] were characterized by x-ray diffraction and magnetization measurements [6]. The temperature dependence of the low field susceptibilities, $\chi_{\parallel}$ ($\mathbf{H} \parallel \hat{\mathbf{c}}$) and $\chi_{\perp}$ ($\mathbf{H} \perp \hat{\mathbf{c}}$), in both materials was found to be nearly isotropic in the paramagnetic phase [see Figs. 1(a) and 1(b)]. The effective paramagnetic moments of Gd and Eu, extracted from high-temperature Curie-Weiss fits, are $8.0\mu_B$ and $7.7\mu_B$, respectively, close to the theoretical value of $7.94\mu_B$, indicating that Gd is trivalent while Eu is divalent. The transition to an AF phase occurs at T_N of 27.1 and 30.8 K in $\mathrm{GdNi_2Ge_2}$ and $\mathrm{EuNi_2Ge_2}$, respectively. Note that T_N for the Gd compound is lower than that of its Eu neighbor. For the Gd compound, $\chi_{\parallel}$ and $\chi_{\perp}$ remain at a similar magnitude until $\chi_{\perp}$ drops drastically below $T_t = 16.8$ K. The additional transition in $\chi_{\parallel}$ at $T_t' = 18.5$ K is not observed in $\chi_{\perp}$ [6]. As the temperature of $\mathrm{EuNi_2Ge_2}$ is lowered through T_N, $\chi_{\parallel}$ continues to

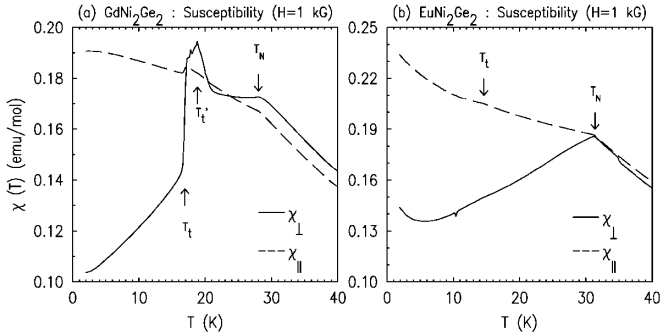

FIG. 1. Temperature dependent magnetic susceptibility of (a) $GdNi_2Ge_2$ and (b) $EuNi_2Ge_2$ compounds.

increase, while $\chi_\perp$ decreases, suggesting an easy plane of magnetization in this compound. A comparison of this behavior to that of $\chi_\parallel$ and $\chi_\perp$ for $GdNi_2Ge_2$ between T_t and T_N suggests an ordered component along the $\hat{\mathbf{c}}$ axis in the latter.

To determine their microscopic magnetic structures, we studied both compounds using the x-ray resonant exchange scattering (XRES) technique, since the neutron opacity of Gd and Eu makes the conventional neutron diffraction methods difficult. $GdNi_2Ge_2$ was studied on the C1 beam line at Cornell High Energy Synchrotron Source (CHESS) with a Si(111) monochromator. No mirror was utilized. A polished rectangular sample was aligned with the $[h\ h\ l]$ zone in the vertical scattering plane. The mosaic at (0 0 6) was $\sim 0.05°$. The incident photon energy was tuned to the L_{II} edge (7.93 keV) of Gd in order to use resonant enhancement [8]. Well above T_N, only charge peaks consistent with the body-centered lattice were observed. At 13 K, careful scans along $\hat{\mathbf{c}}^*$ revealed satellite peaks corresponding to $\mathbf{q}_{\mathrm{Gd}} = (0\ 0\ 0.805)$. The $\mathbf{q}_{\mathrm{Gd}}$ satellites exhibited a dipole ($E1$) resonant behavior a few eV above the L_{II} edge, consistent with their magnetic origin [8]. The ordering wave vector, $\mathbf{q}_{\mathrm{Gd}}$, was found to decrease with increasing temperature continuously to $(0\ 0\ \sim 0.793)$ as T_N was approached, indicating the *incommensurate* nature of the ordering.

The XRES studies of $EuNi_2Ge_2$ were performed on the X22C beam line at the National Synchrotron Light Source (NSLS) described elsewhere [2]. The sample mosaic was similar to that above. At 4.3 K, scans along the $\hat{\mathbf{c}}^*$ axis found superlattice peaks at $\mathbf{q}_{\mathrm{Eu}} = (0\ 0\ 1)$ which showed $E1$ resonant behavior at the Eu L_{II} edge (7.617 keV), remained locked in position up to T_N, and disappeared above T_N. In contrast to the isostructural Tb and Dy compounds [2], we did not observe any other modulations in either Gd or Eu compound.

The $\mathbf{Q}$ dependence [9] of the integrated intensities of magnetic peaks showed [see Figs. 2(a) and 2(b)] the ordered moments to be in the basal plane (solid line) below T_t. However, for $GdNi_2Ge_2$ above T_t but below T_N, there is an ordered component along the $\hat{\mathbf{c}}$ axis which gives additional scattering contribution with a pronounced break at T_t' [Fig. 2(d)]. For a simple spin reorientation in the basal plane, no such break in the intensity above T_t is expected [10]. Rather, the integrated intensity monotonically decreases as in $EuNi_2Ge_2$ [Fig. 2(c)].

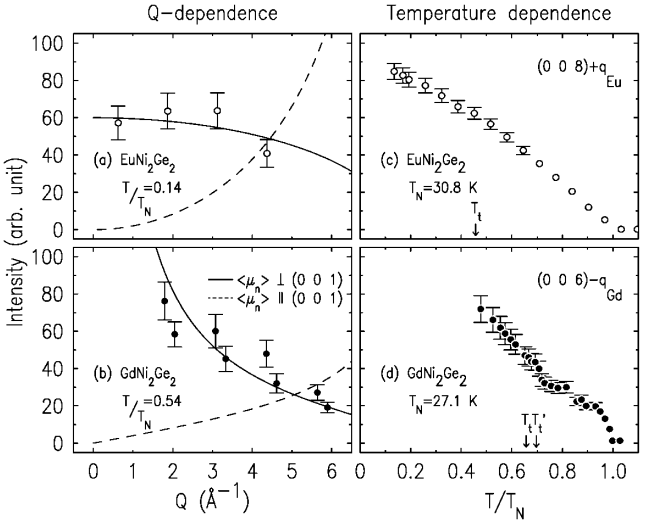

FIG. 2. The $\mathbf{Q}$ dependence of integrated intensities of magnetic peaks ($T < T_t$) for (a) $EuNi_2Ge_2$ and (b) $GdNi_2Ge_2$. Solid line is for a model with the ordered moments $\perp \hat{\mathbf{c}}$ and dashed line is for that with moments $\parallel \hat{\mathbf{c}}$. Data in (a) was normalized by the monitor and that in (b) was normalized by the fluorescence yields. The temperature dependence of a magnetic Bragg peak (as indicated) in (c) $EuNi_2Ge_2$ and (d) $GdNi_2Ge_2$ measured while increasing the temperature.

In order to explain the differences in the ordering wave vector between the Eu and Gd compounds, we now turn to investigations of their electronic structure. In the RKKY theory the exchange energy is proportional to $-|I(\mathbf{q})|^2\chi_0(\mathbf{q})$ [11], where $I(\mathbf{q})$ is the exchange matrix element, neglecting the dependence on the band indices and assuming only $\mathbf{q}$ dependence [12]. Thus, when exchange is the dominant factor in the free energy near the ordering temperature, the wave vector at the onset of ordering is determined by the $\mathbf{q}$ that maximizes $\chi_0(\mathbf{q})$ [assuming small variations in $I(\mathbf{q})$] which is given by [11]

$$\chi_0(\mathbf{q}) = \frac{1}{N}\sum_{n,n',\mathbf{k}} \frac{f(\epsilon_{n,\mathbf{k}})[1 - f(\epsilon_{n',\mathbf{k}+\mathbf{q}+\mathbf{G}})]}{\epsilon_{n',\mathbf{k}+\mathbf{q}+\mathbf{G}} - \epsilon_{n,\mathbf{k}}},$$

where $f(\epsilon)$ is the Fermi-Dirac occupation factor, ϵ's are the electronic energies, n and n' are the band indices, and $\mathbf{G}$ is a reciprocal lattice vector needed to reduce $\mathbf{k} + \mathbf{q}$ to the first Brillouin zone (BZ).

Ab initio local-density-approximation paramagnetic electronic bands were calculated using the tight-binding linear-muffin-tin-orbital method within the atomic sphere approximation (ASA) including combined corrections [13]. The scalar relativistic Schrödinger equation, with the von Barth–Hedin local potential to include the exchange and correlation effects, was solved. The $4f$ electrons were

treated as part of the core. This is consistent with the observed effective moments as well as x-ray photoemission measurements which found the $4f$ level to be ~600 mRyd below the Fermi level (E_f) in $GdNi_2Ge_2$ [14]. The room temperature lattice constants [15] were used in these calculations. $\chi_0(\mathbf{q})$ for $\mathbf{q} = (0\ 0\ q_z)$ was calculated at 0 K using the analytical linear tetrahedron method [16].

Figure 3(a) shows the calculated interband ($A \leftrightarrow B$) susceptibility, $\chi_0^{AB}(\mathbf{q})$ (filled circles), for $GdNi_2Ge_2$ using two bands referred to as A and B which cross E_f. There is a sharp peak at 0.79, very close to the ordering vector with an enhancement of 53% relative to $\chi_0^{AB}(\mathbf{q} \to 0)$. This enhancement is a measure of strength of the peak. The maximum is determined by the dominant interband ($A \leftrightarrow B$) nesting [10]. The nesting vector, $\mathbf{q}_{\text{nest}} = (0\ 0\ 0.79)$, is indicated in Fig. 4 by the vertical arrows. The $\chi_0(\mathbf{q})$ calculations shown here were performed with the Fermi energy shifted upward by 7 mRyd (to E_f'). This changed the peak position in $\chi_0^{AB}(\mathbf{q})$ from 0.86 to 0.79. Such a shift is not unreasonable for band calculations using the ASA, when multiple bands with different orbital character cross E_f [10]. By repeating the calculations, including two more bands near the Fermi level, we found the peak at 0.79 to be the *global* maximum of the total $\chi_0(\mathbf{q})$. The total intraband susceptibility $\chi_0^{\text{intra}}(\mathbf{q} \to 0)$ reached 99.8% of $\frac{1}{2}N(E_f')$, where $N(E_f')$ is the density of states (DOS) at E_f' [10].

Because of the sensitivity of the nesting features to Fermi surface topology, a small shift of the calculated E_f directly affects $\mathbf{q}_{\text{nest}}$. In the elemental rare earths, E_f depends on the $5d$ occupancy which changes with the ionic core volume across the series. This d-band occupancy is responsible for the sequence of crystal structures observed across the rare-earth series [17]. This suggests that small variations of E_f across the RNi_2Ge_2 series may also be responsible for the range of q_z observed (0.75–0.81). Indeed, essentially the entire range of observed q_z exists within ±2.5 mRyd of E_f' and it may be concluded that magnetic ordering in RNi_2Ge_2 with *trivalent* R elements is also driven by Fermi surface nesting. We note, however, that exchange matrix elements and finite temperature can also affect both position and magnitude of the peak of $\chi_0(\mathbf{q})$ [3,18].

Our calculations, so far, are consistent with the experimental findings. To directly observe a correlation between nesting and magnetic ordering, however, we must change the band filling simulating the substitution of Eu^{2+} for Gd^{3+}. Computationally this can be accomplished simply by lowering E_f' by 22 mRyd, corresponding to the removal of exactly "one" electron from $GdNi_2Ge_2$ according to its DOS [10], and calculating $\chi_0(\mathbf{q})$. Figure 3(a) (open squares) presents $\chi_0^{AB}(\mathbf{q})$ calculations with the lower band filling which show a strong sharp peak at the zone boundary, (0 0 1), predicting a *commensurate* simple AF structure in $EuNi_2Ge_2$, as was observed.

Encouraged by this result we have performed $\chi_0(\mathbf{q})$ calculations for $EuNi_2Ge_2$ to confirm the origin of this modulation to be nesting. The results are shown in Fig. 3(b). There is indeed a sharp peak at $q_z = 1$ which is also the *global* maximum [10]. As in the Gd case, the $\chi_0^{AB}(\mathbf{q})$ shown is obtained with E_f shifted upward (to $E_f'' = E_f + 10$ mRyd). The peak in $\chi_0^{AB}(\mathbf{q})$ due to interband ($A \leftrightarrow B$) nesting occurs at the zone boundary (see Fig. 4) for $E_f'' \pm 2$ mRyd. Furthermore, this peak shifts

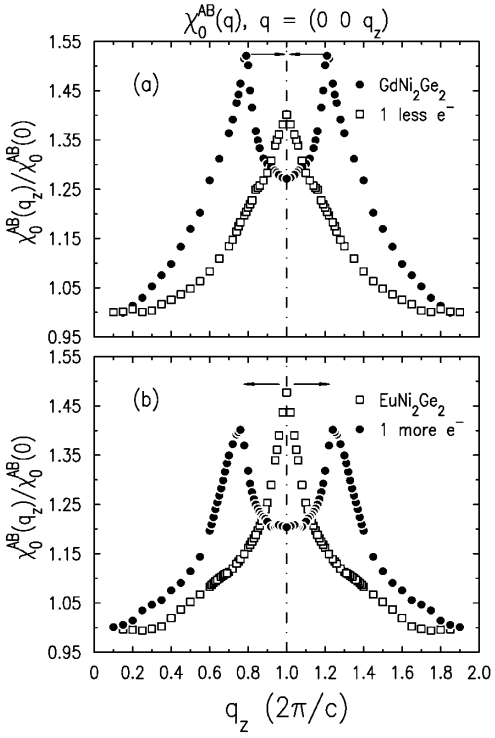

FIG. 3. Interband generalized electronic susceptibility, $\chi_0^{AB}(\mathbf{q})$. See text for details.

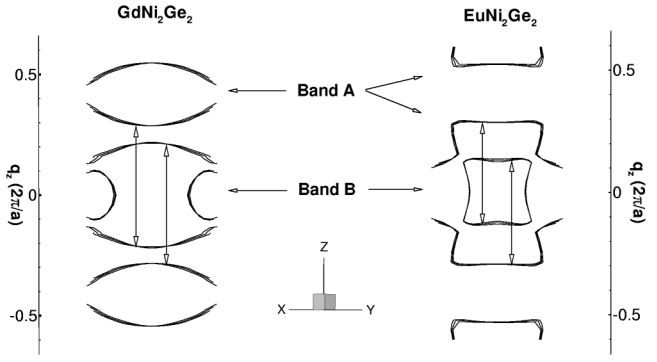

FIG. 4. Interband ($A \leftrightarrow B$) nesting in $GdNi_2Ge_2$ and $EuNi_2Ge_2$. A and B form a nested pair of "saddles" over a considerable region. Contour plots on three parallel planes [⊥[1 1 0], with the origins near (0.15 0.15 0)] of a portion of such regions with $\mathbf{q}_{\text{nest}}$ indicated by the arrows. Because of fourfold symmetry, there are four such nested regions. $\mathbf{q}_{\text{nest}}$ for $GdNi_2Ge_2$ needs to be reduced to the first BZ. Note that the unit used for q_z is $\frac{2\pi}{a}$.

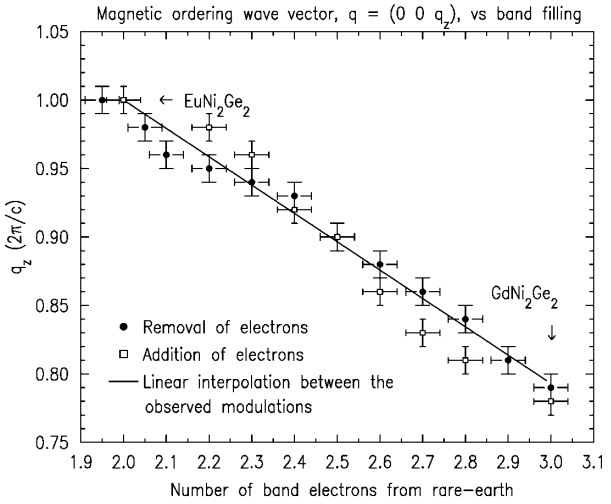

FIG. 5. Predicted modulation vectors obtained from the peak position of $\chi_0(\mathbf{q})$ as a function of band filling.

to 0.78 with the addition of one electron (corresponding to $E_f'' + 23$ mRyd obtained from DOS of $EuNi_2Ge_2$ [10]), in excellent agreement with that for $GdNi_2Ge_2$.

We note that up to this point we have ignored the fact that the lattice constants of $EuNi_2Ge_2$ are $\sim$3% larger than those of $GdNi_2Ge_2$ [15]. In order to assess the influence of this difference upon the nesting we repeated all the band and $\chi_0(\mathbf{q})$ calculations by swapping the lattice parameters between the two compounds. These calculations found *no* significant changes in the conclusions reached above [10].

Based on the above analysis we note that it may be possible to transform the incommensurate structure observed in $GdNi_2Ge_2$ into the commensurate AF phase found in $EuNi_2Ge_2$ by lowering the band filling. Figure 5 shows the ordering vector obtained from the peak in $\chi_0(\mathbf{q})$ calculated by removing electrons from $GdNi_2Ge_2$ as well as by adding electrons to $EuNi_2Ge_2$. Interestingly, calculated q_z values lie close to the linear interpolation between the experimentally observed modulations of the end members. Future experiments with XRES on $Gd_{1-x}Eu_xNi_2Ge_2$ pseudoternary alloys are suggested to explore these predictions and to determine at which finite Gd content a locking to (0 0 1) will occur.

Finally, we turn to the issue of the higher T_N found for $EuNi_2Ge_2$ relative to $GdNi_2Ge_2$. In general, T_N scales with the product $\langle I \rangle^2 \chi_0(\mathbf{q})$. Since the Néel transition is driven by interband ($A \leftrightarrow B$) nesting, we have estimated the interband exchange matrix element, $\langle I_{AB} \rangle$, by considering the product $|C_{5d}^A(\mathbf{k})| \cdot |C_{5d}^B(\mathbf{k} + \mathbf{q}_{\text{nest}})|$ where C_{5d} is the amount of $5d$ character of a band electron. We find that, on average, $\frac{\langle I_{AB}(EuNi_2Ge_2) \rangle^2}{\langle I_{AB}(GdNi_2Ge_2) \rangle^2} \sim 1.3$. Also, $\chi_0^{AB}(\mathbf{q}_{\text{Eu}})$ and $\chi_0^{AB}(\mathbf{q}_{\text{Gd}})$ are 29.35 and 23.69 [states/(Ryd cell)], respectively. Therefore, we argue that T_N in $EuNi_2Ge_2$ is higher due to larger values of these two quantities.

We thank J. P. Hill for his intellectual contributions and critical reading of the manuscript, and acknowledge S. Coburn and B. Schoenig for their technical assistance at NSLS. Ames Laboratory (DOE) is operated by Iowa State University under Contract No. W-7405-Eng-82. This work was supported by the Director for Energy Research, Office of Basic Sciences. The work at NSLS (BNL) was carried out under Contract No. DEAC0298-CH10886, Division of Materials Science (DOE). CHESS is supported by the National Science Foundation (NSF). This work was supported, in part, by NSF ALCOM Grant No. DMR89-20147.

*Present address: Department of Physics, Northern Illinois University, DeKalb, IL; Advanced Photon Source, Argonne National Laboratory, Argonne, IL.
Email address: zahir@aps.anl.gov
†Present address: ESRF, Grenoble, France.

[1] A. Szytuła *et al.*, *Handbook of Crystal Structures and Magnetic Properties of Rare Earth Intermetallics* (CRC, Boca Raton, FL, 1994), pp. 114–192.
[2] Z. Islam *et al.* Phys. Rev. B **58**, 8522 (1998); Solid State Commun. **108**, 371 (1998); National Synchrotron Light Source Annual Report 1998; preliminary XRES studies at 4 K on $SmNi_2Ge_2$ (unpublished).
[3] W. E. Evenson and S. H. Liu, Phys. Rev. Lett. **21**, 432 (1968); Phys. Rev. **178**, 432 (1969).
[4] S. Legvold *et al.*, Solid State Commun. **21**, 1061 (1976).
[5] H.-J. Hesse *et al.*, J. Alloys Compd. **246**, 220 (1997).
[6] S. L. Bud'ko *et al.*, J. Magn. Magn. Mater. (to be published).
[7] P. C. Canfield and Z. Fisk, Philos. Mag. B **56**, 1117 (1992).
[8] J. P. Hannon *et al.*, Phys. Rev. Lett. **61**, 1245 (1988); D. Gibbs *et al.*, Phys. Rev. Lett. **61**, 1241 (1988).
[9] J. P. Hill and D. F. McMorrow, Acta. Crystallogr. Sect. A **5**, 236 (1996); C. Detlefs, Ph.D. thesis, Iowa State University, 1997.
[10] Z. Islam, Ph.D. thesis, Iowa State University, 1999.
[11] S. Liu, in *Handbook on the Physics and Chemistry of Rare Earths*, edited by K. Gschneidner and L. Eyring (North-Holland, Amsterdam, 1978), Vol. 1.
[12] R. E. Watson *et al.*, Phys. Rev. **152**, 566 (1966); *ibid.* **178**, 725 (1969); B. N. Harmon *et al.*, Phys. Rev. B **10**, 4849 (1974).
[13] O. K. Anderson, in *Highlights of Condensed-Matter Theory*, edited by F. Bassani *et al.* (North-Holland, Amsterdam, 1985), p. 59.
[14] D. Brammeier and D. Lynch (private communication).
[15] W. Rieger *et al.*, Monat. für Chemie **100**, 444 (1969).
[16] J. Rath *et al.*, Phys. Rev. B **11**, 2109 (1975).
[17] J. C. Duthie *et al.*, Phys. Rev. Lett. **38**, 564 (1977).
[18] R. P. Gupta and S. K. Sinha, Phys. Rev. B **3**, 2401 (1971); J. Appl. Phys. **41**, 915 (1970); K. Grobsky and B. N. Harmon, J. Appl. Phys. **49**, 2147 (1978).